Nicotinic acetylcholine receptor agonist reduces acute lung injury after renal ischemia-reperfusion injury by acting on splenic macrophages in mice

メタデータ	言語: English
	出版者: The American Physiological Society
	公開日: 2023-02-15
	キーワード (Ja):
	キーワード (En): acute kidney injury, acute lung injury, macrophage, nicotinic acetylcholine receptor agonist
	作成者: 後藤, 大樹
	メールアドレス:
	所属:
URL	http://hdl.handle.net/10271/00004268

AMERICAN JOURNAL OF PHYSIOLOGY

RENAL PHYSIOLOGY®

RESEARCH ARTICLE

Inter-Organ Communication in Homeostasis and Disease

Nicotinic acetylcholine receptor agonist reduces acute lung injury after renal ischemia-reperfusion injury by acting on splenic macrophages in mice

Daiki Goto,[1] Soichiro Nagata,[1] Yoshitaka Naito,[1] Shinsuke Isobe,[1] ⓘ Takamasa Iwakura,[1] Tomoyuki Fujikura,[1] Naro Ohashi,[1] Akihiko Kato,[2] Hiroaki Miyajima,[1] Ken Sugimoto,[1] and ⓘ Hideo Yasuda[1]

[1]*First Department of Medicine, Hamamatsu University School of Medicine, Hamamatsu, Japan and* [2]*Division of Blood Purification, Hamamatsu University Hospital, Hamamatsu, Japan*

Abstract

Acute kidney injury (AKI) contributes to the development of acute lung injury (ALI) via proinflammatory responses. We hypothesized that activation of a nicotinic acetylcholine receptor (nAChR), which exerts cholinergic anti-inflammatory effects on macrophages, could reduce ALI after AKI. We aimed to determine whether nAChR agonists could reduce ALI after AKI and which macrophages in the lung or spleen contribute to the improvement of ALI by nAChR agonists. We induced AKI in male mice by unilateral ischemia-reperfusion injury (IRI) with contralateral nephrectomy and administered nAChR agonists in three experimental settings: *1*) splenectomy, *2*) deletion of splenic macrophages and systemic mononuclear phagocytes via intravenous administration of clodronate liposomes, and *3*) alveolar macrophage deletion via intratracheal administration of clodronate liposomes. Treatment with GTS-21, an α7nAChR-selective agonist, significantly reduced the levels of circulating IL-6, a key proinflammatory cytokine, and lung chemokine (C-X-C motif) ligand (CXCL)1 and CXCL2 and neutrophil infiltration, and Evans blue dye (EBD) vascular leakage increased after renal IRI. In splenectomized mice, GTS-21 did not reduce circulating IL-6 and lung CXCL1 and CXCL2 levels and neutrophil infiltration, and EBD vascular leakage increased after renal IRI. In mice depleted of splenic macrophages and systemic mononuclear phagocytes, GTS-21 treatment did not reduce lung neutrophil infiltration, and EBD vascular leakage increased after renal IRI. In mice depleted of alveolar macrophages, GTS-21 treatment significantly reduced lung neutrophil infiltration, and EBD vascular leakage increased after renal IRI. Our findings show that nAChR agonist reduces circulating IL-6 levels and acute lung injury after renal IRI by acting on splenic macrophages.

NEW & NOTEWORTHY Acute lung injury associated with acute kidney injury contributes to high mortality. This study showed, for the first time, that nicotinic acetylcholine receptor agonists reduced circulating IL-6 and ALI after renal ischemia-reperfusion injury in mice. These effects of α7nAChR agonist were eliminated in both splenectomized and splenic macrophage (including systemic mononuclear phagocyte)-depleted mice but not alveolar macrophage-depleted mice. nAChR agonist could reduce ALI after AKI via splenic macrophages and provide a novel strategy in AKI.

acute kidney injury; acute lung injury; macrophage; nicotinic acetylcholine receptor agonist

INTRODUCTION

Acute kidney injury (AKI) is characterized by rapid deterioration of renal function, which is associated with ∼12% of patients being hospitalized and ∼50% of these admitted to the intensive care unit (1, 2). Complications of AKI worsen the prognosis of hospitalized patients (3). High-intensity renal replacement therapy and early renal replacement therapy do not improve the prognosis of patients with AKI (4, 5), suggesting that there are other factors that influence mortality in addition to decreased clearance of uremic toxins. Distant organ damage with concomitant AKI may contribute to high mortality (6, 7). Mortality in patients with AKI

requiring renal replacement therapy increases from 40–50% to 60–80% due to complications of distant organ damage (8, 9). In particular, acute lung injury (ALI) associated with AKI is thought to contribute to the worsening of prognosis (10–12). Thus, ALI associated with AKI is an important therapeutic target in patients with AKI.

The development of ALI after AKI has been shown to contribute to both hydrostatic and nonhydrostatic edema (13). One of the causes of nonhydrostatic edema is systemic inflammation caused by IL-6, IL-8, and TNF-α (14–17). In particular, circulating IL-6 plays a central role in ALI development after AKI (15). The major organs that produce IL-6 after AKI could be the spleen and liver in addition to the kidney,

http://www.ajprenal.org

and macrophages could be a major producing cell of IL-6 production after AKI (14, 17, 18). Depletion of macrophages reduces lung inflammation after AKI (14, 19). Taken together, this indicates that splenic macrophages may play an important role in the development of ALI after AKI. The anti-inflammatory mechanism of action of splenic macrophages might improve ALI after AKI.

Nicotine, an acetylcholine (ACh) receptor agonist, and 3-(2,4-dimethoxy-benzylidene)-anabaseine dihydrochloride (GTS-21), an α7-nicotinic ACh receptor (α7nAChR)-selective agonist, bind to α7nACRs of macrophages in the spleen and suppress the production of proinflammatory cytokines such as TNF-α and IL-6 to exert an anti-inflammatory effect (20, 21). The activation of α7nACRs of macrophages in the spleen plays an important role in the cholinergic anti-inflammatory pathway (CAP) (22–24), by which vagus nerve stimulation protects organs from injuries, including ventilator-induced lung injury (25). We hypothesized that α7nAChR agonists have anti-inflammatory effects that act on splenic macrophages and improve ALI after AKI.

Both alveolar macrophages as well as splenic macrophages contain α7nAChRs (26), and the systemic administration of α7nAChR agonists could act on macrophages in both the spleen and lungs. It has been reported that depletion of both systemic and alveolar macrophages reduces lung inflammation after AKI but exacerbates lung capillary leakage (14). It has not yet been determined whether both splenic and alveolar macrophages could mediate ALI after AKI. To clarify which macrophages predominantly mediate ALI after AKI in our experimental setting, the effects of α7nAChR agonists were evaluated in mice depleted of systemic mononuclear phagocytes including splenic macrophages or alveolar macrophages via intravenous or intratracheal administration of clodronate liposomes.

In this study, we aimed to verify the hypothesis that α7nAChR agonists improve ALI after AKI using a renal ischemia-reperfusion injury (IRI) model and examined the involvement of splenic macrophages and alveolar macrophages in the mechanism of action of α7nAChR agonists.

MATERIALS AND METHODS

Nicotinic AChR Agonist

($-$)-Nicotine (Cat. No. N3876), a nonselective nicotinic AChR agonist, was obtained from Sigma-Aldrich (St. Louis, MO). GTS-21 (Cat. No. ab120560) was obtained from Abcam (Cambridge, UK). Before experimentation, nicotine was diluted with 0.9% saline, and GTS-21 was dissolved in PBS. Saline (0.9%) and PBS were used as vehicles for nicotine and GTS-21, respectively.

Antibody

Anti-mouse CD64 FITC (Cat. No./Clone: 139316/X54-5/7.1), anti-mouse F4/80 PE (Cat. No./Clone: 123109/BM8), anti-mouse CD11c APC (Cat. No./Clone: 117309/N418), anti-mouse CD11b APC-Cy7 (Cat. No./Clone: 101225/M1/70), anti-mouse CD45 Pacific blue (Cat. No./Clone: 103125/30-F11), and appropriate isotype control antibodies were obtained from BioLegend (San Diego, CA).

Animal Preparation

Seven- to eight-week-old C57BL6/J male mice were obtained from SLC Japan (Hamamatsu, Japan) for all experiments. Mice were bred in a standard laboratory environment (temperature: 24 ± 2°C, humidity: 55 ± 5%, 12:12-h light-dark cycle) with free access to water and food. All protocols were approved by the Ethics Committee for Animal Experiments of Hamamatsu University School of Medicine (Approval No. 2019022).

Unilateral Nephrectomy With or Without Splenectomy

Mice were anesthetized with 5% sevoflurane. A right flank incision was made, and the right kidney was removed after ligation of the right renal hilum. When splenectomy was performed at the same time, a midline abdominal incision was made, after which the left kidney and spleen were removed after ligation of the left renal hilum and splenic vasculature. After skin closure, mice received 0.25 mg/kg body wt buprenorphine as an analgesic. Mice were allowed to recover for 2 wk before the renal IRI experiments.

Renal Unilateral IRI

Mice were anesthetized with three anesthetics: medetomidine hydrochloride (0.3 mg/kg body wt), midazolam (4 mg/kg body wt), and butorphanol tartrate (5 mg/kg body wt). During the operation, rectal temperature was maintained at 37°C–38°C using a heat pad and an infrared lamp. Kidney unilateral IRI was performed through the left or right flank incision by clamping the left or right renal hilum with a cerebral aneurysm clip for 35 min. The clamp was removed, and the kidney color changed from black to red. After skin closure, mice received 0.25 mg/kg body wt buprenorphine as an analgesic and were woken from anesthesia with atipamezole hydrochloride (0.3 mg/kg body wt). Sham-operated mice underwent the same procedure except for clamping the left or right renal hilum.

Experiment Groups

Mice were divided into the following four groups: sham-operated + vehicle group, sham-operated + α7nACh agonist group, IRI + vehicle group, and IRI + α7nACh agonist group. The sham-operated groups underwent right nephrectomy or right nephrectomy and splenectomy + sham IRI. The IRI group underwent right nephrectomy or right nephrectomy and splenectomy + IRI. Mice received α7nACh agonists [nicotine (1 mg/kg) or GTS-21 (4 mg/kg)] or vehicles 5 and 0.5 h before reperfusion (27, 28). Mice were euthanized with an overdose of sevoflurane 2 or 24 h after reperfusion. The evaluation points were determined by referring to the preliminary experiments and previous reports (Supplemental Fig. S1; all Supplemental Material is available at https://doi.org/10.6084/m9.figshare.16608162.v1) (16, 18).

Measurement of Plasma Creatinine Levels

Blood samples were collected via cardiac puncture and centrifuged at 4°C at 8,000 rpm for 10 min. Plasma creatinine levels were measured using enzymatic assays conducted by Sanritsu Zelkova Laboratory (Kanagawa, Japan).

Homogenization of Lung Tissue

The frozen right lobe of the lung was homogenized on ice in 280 μL PBS with 1% protease inhibitor cocktail (Cat. No. 11836153001) obtained from Roche (Mannheim, Germany). Subsequently, 70 μL of 5% Triton X-100 in PBS was added to the sample, and the sample was vortexed and incubated on ice for 20 min. Samples were then centrifuged at 4°C and 14,000 g for 15 min. Lysates were stored at −80°C until protein and cytokine measurements (29).

Measurement of Plasma and Pulmonary Proinflammatory Cytokines

Plasma and pulmonary IL-6 and TNF-α and pulmonary IL-10 levels were determined using ELISA kits (Cat. Nos. M6000B, MTA00B, MKC00B, MM200, M1000B, and ab1007143) obtained from R&D Systems (Minneapolis, MN) and Abcam according to the manufacturer's instructions. Protein concentrations in the pulmonary lysate were measured using a protein assay kit (Cat. No. 30181002) obtained from WAKO (Osaka, Japan) according to the manufacturer's instructions. Pulmonary cytokine levels were calculated as cytokine concentration/protein concentration.

Renal Histology

The left kidneys were fixed in 10% formalin for 24 h, embedded in paraffin, and cut into 4-μm sections to prepare them for periodic acid-Schiff staining. The percentages of necrotic tubules were calculated by an investigator who was blinded to the experimental groups in 10 nonoverlapping areas randomly selected in the outer stripe of the outer medulla (OSOM) at ×400 magnification in the respective sections of each kidney and averaged (30).

Lung Histology

Whole lungs fixed with 10% formalin for 24 h were embedded in paraffin and cut into 4-μm sections. They were then prepared for hematoxylin and eosin staining. Neutrophils were counted by an investigator who was blinded to the experimental groups, and the data were averaged from 20 nonoverlapping areas randomly selected at ×400 magnification in the respective sections of each lung (31).

Vascular Permeability Assay Using Evans Blue Dye

Vascular permeability was evaluated using Evans blue dye (EBD; Cat. No. E2129) obtained from Sigma-Aldrich. This assay is a well-established method for determining noncardiogenic pulmonary edema (18, 32). Briefly, 250-μL EBD (5 mg/mL) was injected into the retroorbital sinus 1 h before the mice were euthanized. To remove EBD within the vasculature, the lungs were perfused with 5-mL PBS via the right ventricle. The harvested lungs were weighed and homogenized in 1-mL formamide. The homogenate was incubated overnight at 37°C and then centrifuged at 10,000 g for 30 min. Absorbance at 620 nm (A620) and 740 nm (A740) of the supernatant was determined. The value of A620 was corrected for the presence of heme pigments using the following formula: A620 (corrected) = A620 − (1.426 × A740 + 0.030). The EBD content in the lungs was calculated by comparison with a standard curve. The results were expressed as micrograms of EBD per gram of organ tissue (wet weight).

Reduction of Macrophages

Clodronate liposomes (Clophosome, Cat. No. F70101C-N) obtained from FormuMax (Sunnyvale, CA) was used to reduce macrophages. To reduce splenic macrophages including systemic mononuclear phagocytes, 150 μL of clodronate liposomes were injected into the retroorbital sinus 1 day before IRI. For the reduction of alveolar macrophages, 40 μL of clodronate liposomes were administered intratracheally once per day for 3 days before IRI (33). Control liposomes obtained from the same source were used in all experiments.

Identification of Spleen Macrophages (Red Pulp Macrophages) and Alveolar Macrophages by Flow Cytometry

Mice were perfused with 5-mL PBS before the lungs and spleen were harvested. Spleens were minced with a syringe on a 70-μm nylon cell strainer (Cat. No. 352350) obtained from Falcon (Corning, NY). Cell suspensions were washed and passed through 40-μm nylon cell strainers (Cat. No. 352340) obtained from Falcon. The lungs were incubated with 2 mg/mL collagenase type 2 (Cat. No. LS004176, Worthington, Lakewood, NJ) and 0.1 mg/mL DNase 1 (Worthington) for 30 min at 37°C in PBS. Digested lung tissues were then cut using a gentleMACS Dissociator (Miltenyi Biotechnology, Bergisch Gladbach, Germany) according to the manufacturer's instructions. Cell suspensions were washed and filtered through 40-μm cell strainers. Red blood cells were excluded from the spleen and lung cells using lysis buffer (Cat. No. 130-094-183) obtained from Miltenyi Biotechnology. Single cell suspensions were labeled with antibodies after incubation with BD PharMingen (Cat. No. 553142) obtained from BD Biosciences (Franklin Lakes, NJ) to reduce nonspecific binding. To identify spleen macrophages (red pulp macrophages) or alveolar macrophages, cell phenotyping was performed (Supplemental Fig. S2, A and B) using a Gallios Flow Cytometer (Beckman Coulter, Brea, CA) (34, 35). First, doublet cells were excluded by FSC-W and FSC-A discrimination, and the distinction between living and dead cells was made using 7-aminoactinomycin D (Cat. No. 7240-37-1) from Sigma-Aldrich. Next, CD45$^+$ immune cells were gated from the living singlet cells. Finally, red pulp macrophages and alveolar macrophages were gated from CD45$^+$ immune cells. Red pulp macrophages were characterized as CD64$^+$ F4/80$^+$ and alveolar macrophages were characterized as F4/80$^+$ CD11c$^+$ CD11b$^-$. The number of macrophages was calculated for the whole spleen or lung using CountBright (Cat. No./Lot C36950/2162689) obtained from Invitrogen (Waltham, MA). The results were analyzed using FlowJo software (Tree Star, Ashland, OR).

Statistical Analyses

Results are expressed as means ± SD. Differences between two groups were analyzed using an unpaired t test or Mann–Whitney test, and differences among four groups were analyzed using two-way ANOVA followed by Tukey's

multiple-comparisons test or Bonferroni's multiple-comparisons test. All statistical calculations were performed using GraphPad Prism 9 software (GraphPad, La Jolla, CA).

RESULTS

α7nAChR Agonists Reduce Lung Injury After Renal IRI

Nicotine (1 mg/kg) was administered to mice at 5 and 0.5 h before reperfusion as a α7nAChR agonist (Fig. 1A). The lungs

of mice that underwent renal IRI were heavily infiltrated with neutrophils after 2 h [IRI + saline vs. sham + saline: 17.1 ± 4.47 vs. 4.8 ± 2.44 cells/high-powered field (HPF), $P <$ 0.0001, Fig. 1, B and C]. Administration of nicotine significantly reduced the number of neutrophil infiltrations into the lung (IRI + nicotine vs. IRI + saline: 11.4 ± 4.16 vs. 17.1 ± 4.47 cells/HPF, $P <$ 0.01, Fig. 1, B and C). Vascular permeability 24 h after reperfusion was significantly diminished by the administration of nicotine (IRI + nicotine vs. IRI + saline: 11.82 ± 2.415 vs. 19.23 ± 6.604 µg/g lung tissue, $P <$
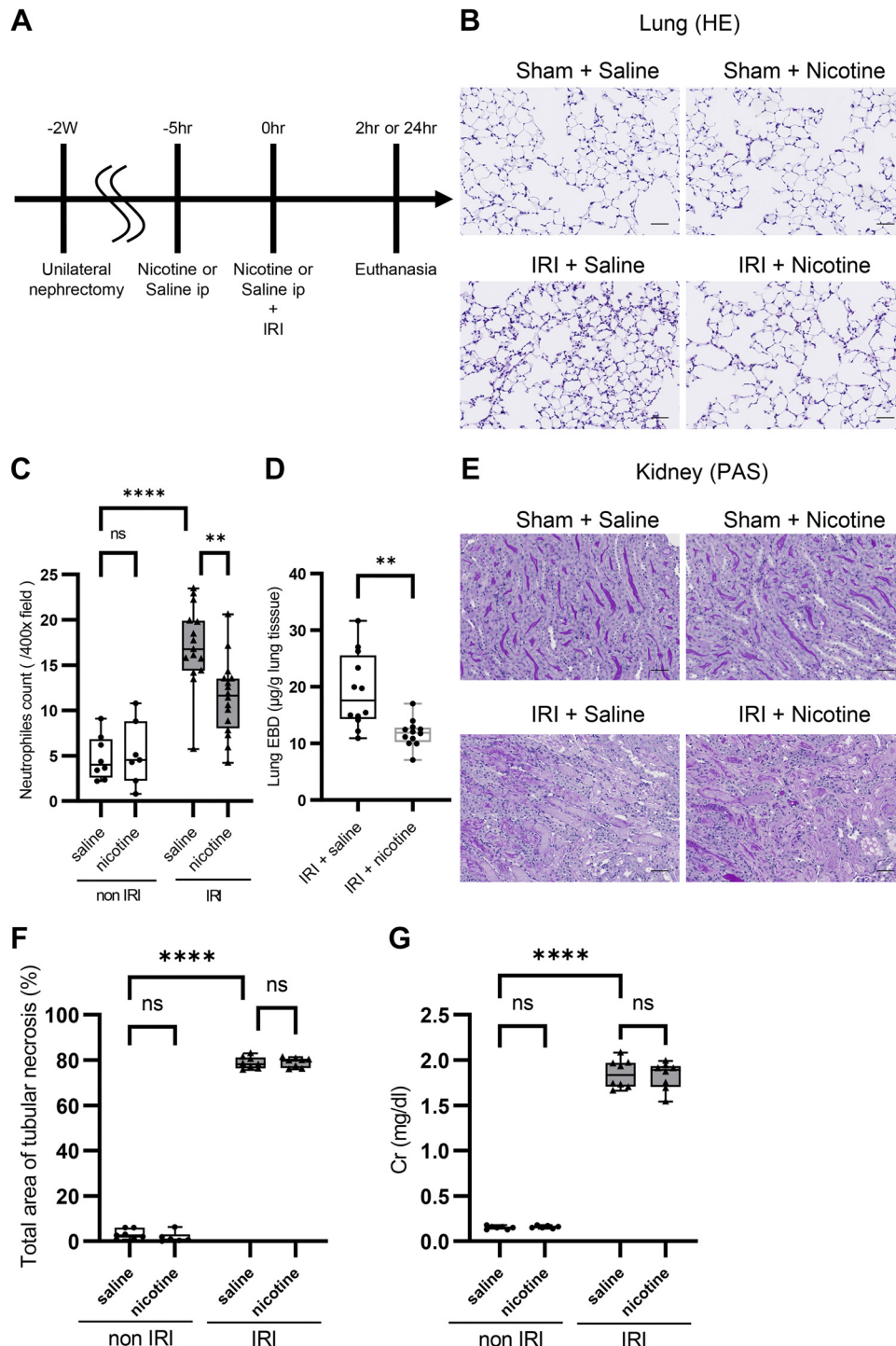

Figure 1. Nicotine reduced lung neutrophil infiltration 2 h after ischemia-reperfusion injury (IRI) and lung Evans blue dye (EBD) leakage 24 h after IRI but did not decrease plasma creatinine (Cr) levels and necrosis area in the kidney 24 h after IRI. *A*: experiment protocol. *B*: representative images of hematoxylin and eosin (HE)-stained lung tissue. *C*: neutrophil infiltration in the lung 2 h after IRI (*n* = 15 or 16 in the IRI group and *n* = 7 or 8 in the sham group). *D*: lung EBD leakage 24 h after IRI (*n* = 12/group). *E*: representative images of periodic acid-Schiff (PAS)-stained renal tissue. *F*: the percentage of necrotic tubules in the outer stripe of the outer medulla in the kidney 24 h after IRI (*n* = 6–8/group). *G*: plasma Cr levels 24 h after IRI (*n* = 6–8/group). The data set in *D* was analyzed by an unpaired *t* test. The other data sets were analyzed by two-way ANOVA followed by Tukey's multiple-comparisons tests. Individual data are shown as dots. The *top*, *middle*, and *bottom* lines indicate the 75th, 50th, and 25th percentile values, respectively. Whiskers indicate the minimum to maximum values. **$P <$ 0.01 and ****$P <$ 0.0001. Scale bars = 50 µm. ns, not significant.

0.01, Fig. 1D). The necrotic area in the kidney and plasma creatinine increased 24 h after reperfusion (necrotic area: IRI + saline vs. sham + saline, 78.8 ± 2.64% vs. 3.1 ± 2.04%, $P < 0.0001$, Fig. 1, E and F; plasma creatinine: IRI + saline vs. sham + saline, 1.85 ± 0.156 vs. 0.15 ± 0.018 mg/dL, $P < 0.0001$, Fig. 1G). Nicotine administration did not reduce the necrotic area in the kidney and plasma creatinine 24 h after reperfusion [necrotic area: IRI + nicotine vs. IRI + saline, 78.9 ± 2.13% vs. 78.8 ± 2.64%, P = not significant (NS), Fig. 1, E and F; plasma creatinine: IRI + nicotine vs. IRI + saline, 1.83 ± 0.152 vs. 1.85 ± 0.156 mg/dL, P = NS, Fig. 1G].

Nicotine is a nonselective agonist that binds to any subunit of the nicotine receptor. The nAChR consists of nine types of α (α2−α9) and three types of β (β2−β4) subunits, and there are homomeric (α7 or α9) and heteromeric (α2−α6 with β2 − β4) subtypes (36). Heteromeric subtypes are also present in lung epithelial cells, among which α3β2α5nAChR attenuates signals through α7nAChRs (37). It has also been reported that the α9 homomeric subunit exists in most immune cells (36). Therefore, to confirm that the ALI protective effect of nicotine is mediated by α7nAChR, further verification was performed using GTS-21, an α7nAChR-selective agonist. GTS-21 was administered to mice 5 and 0.5 h before reperfusion (Fig. 2A). In the lungs of mice treated with GTS-21, the number of neutrophil infiltrates into the lungs 2 h after reperfusion was significantly reduced (IRI + GTS-21 vs. IRI + PBS: 11.7 ± 2.55 vs. 23.0 ± 3.56 cells/HPF, $P < 0.0001$, Fig. 2, B and C), and vascular permeability 24 h after reperfusion was significantly diminished (IRI + GTS-21 vs. IRI + PBS: 8.04 ± 3.359 vs. 13.54 ± 5.475 μg/g lung tissue, $P < 0.01$, Fig. 2D). Pulmonary cytokines including IL-6, TNF-α, chemokine (C-X-C motif) ligand (CXCL)1, CXCL2, and IL-10 (Fig. 2, E–I), and plasma cytokines, including IL-6, TNF-α, CXCL1, and IL-10 (Fig. 2, J–M) were measured at 2 and 24 h after operation. Administration of GTS-21 significantly reduced pulmonary CXCL1 and CXCL2 levels 2 h after renal IRI (CXCL1: IRI + GTS-21 vs. IRI + PBS: 1,036 ± 256.5 vs. 1,631 ± 755.2 pg/mg protein, $P < 0.05$, Fig. 2G; CXCL2: IRI + GTS-21 vs. IRI + PBS: 69.3 ± 50.54 vs. 267.6 ± 342.5 pg/mg protein, $P < 0.05$, Fig. 2H), although it did not change the other pulmonary cytokine levels (Fig. 2, E, F, and I). GTS-21 administration significantly reduced plasma IL-6 levels 2 h after renal IRI (IRI + GTS-21 vs. IRI + PBS: 1,311 ± 1,150 vs. 4,044 ± 5,798 pg/mL, $P < 0.05$, Fig. 2J) but did not alter the levels of other plasma cytokines (Fig. 2, K–M). Administration of GTS-21 did not reduce the necrotic area in the kidney and plasma creatinine 24 h after reperfusion (necrotic area: IRI + GTS-21 vs. IRI + PBS: 81.4 ± 3.76% vs. 78.3 ± 5.06%, P = NS, Supplemental Fig. S3, A and B; plasma creatinine: IRI + GTS-21 vs. IRI + PBS: 1.83 ± 0.278 vs. 1.78 ± 0.336 mg/dL, P = NS, Supplemental Fig. S3C).

GTS-21 Did Not Reduce Lung Injury After Renal IRI Without the Spleen

Splenectomy was performed 2 wk before IRI to investigate whether the spleen contributed to the protective effect of GTS-21 on lung injury after renal IRI (Fig. 3A). The lungs of splenectomized mice that underwent renal IRI were heavily infiltrated with neutrophils after 2 h (IRI + PBS vs. sham + PBS: 46.4 ± 17.80 vs. 23.7 ± 13.45 cells/HPF, $P < 0.05$, Fig. 3, B and C). In contrast to mice with spleens, GTS-21 did not

reduce the number of neutrophil infiltrates into the lung at 2 h and vascular permeability at 24 h after reperfusion (neutrophil infiltration: IRI + GTS-21 vs. IRI + PBS: 37.5 ± 13.80 vs. 46.4 ± 17.80 cells/HPF, P = NS, Fig. 3, B and C; vascular permeability: IRI + GTS-21 vs. IRI + PBS: 22.18 ± 10.980 vs. 23.30 ± 9.358 μg/g lung tissue, P = NS, Fig. 3D) in splenectomized mice. Unlike in the case of mice with spleens, GTS-21 did not change the levels of pulmonary cytokines (Fig. 3, E–I) or plasma cytokines (Fig. 3, J–M). The necrotic area in the kidney and plasma creatinine 24 h after reperfusion increased in IRI-treated mice (necrotic area: IRI + PBS vs. sham + PBS: 79.3 ± 3.71% vs. 0.1 ± 0.16%, $P < 0.0001$, Supplemental Fig. S4, A and B; plasma creatinine: IRI + PBS vs. sham + PBS: 1.96 ± 0.051 vs. 0.17 ± 0.008 mg/dL, $P < 0.0001$, Supplemental Fig. S4C). There was no reduction in the necrotic area in the kidney and plasma creatinine in the presence of GTS-21 at 24 h after renal IRI (necrotic area: IRI + GTS-21 vs. IRI + PBS: 79.4 ± 2.36% vs. 79.3 ± 3.71%, P = NS, Supplemental Fig. S4, A and B; plasma creatinine: IRI + GTS-21 vs. IRI + PBS: 79.4 ± 2.36% vs. 79.3 ± 3.71%, P = NS, Supplemental Fig. S4C).

GTS-21 Did Not Reduce Lung Injury After Renal IRI Under Deletion of Splenic Macrophages and Systemic Mononuclear Phagocytes

To confirm that GTS-21 reduced lung injury after renal IRI via splenic macrophages, splenic macrophages and systemic mononuclear phagocytes were removed by intravenous administration of 150 μL of clodronate liposomes 1 day before renal IRI (Fig. 4A). The intravenous administration of clodronate liposomes dramatically reduced the red pulp macrophage count in the spleen compared with vehicle administration (clodronate vs. control: 0.34 ± 0.251 vs. 1.14 ± 0.363 × 10⁶ cells/whole spleen, $P < 0.001$, Fig. 4B) but not alveolar macrophage count (clodronate vs. control: 8.47 ± 1.408 vs. 8.30 ± 1.256 × 10⁵ cells/whole lung, P = NS, Fig. 4C). Resident macrophages in the spleen are thought to have subtypes of red pulp macrophages, marginal zone macrophages, marginal zone metallophilic macrophages, and white pulp macrophages (38). The expression of surface markers differs depending on the subtype, and it has been reported that F4/80 is strongly expressed in red pulp macrophages, but F4/80 is weakly expressed in tingible body macrophages in the white pulp of the spleen (39). In this study, the elimination of red pulp macrophages was confirmed by flow cytometry, but the elimination of other subtypes of macrophages was not confirmed using surface markers characteristic of other subtypes. However, Rosas-Ballina et al. (24) have previously reported that red pulp macrophages produce TNF-α during endotoxinemia and that the production is suppressed by nicotine and that it is reasonable to consider red pulp macrophages as a target for nAChR agonists even in IRI.

The lungs in mice without splenic macrophages and systemic mononuclear phagocytes were heavily infiltrated with neutrophils 2 h after renal IRI (IRI + PBS vs. sham + PBS: 37.0 ± 11.27 vs. 11.3 ± 8.50 cells/HPF, $P < 0.001$, Fig. 4, D and E). GTS-21 did not reduce lung neutrophil infiltration at 2 h or vascular permeability at 24 h after reperfusion (neutrophil infiltration: IRI + GTS-21 vs. IRI + PBS: 34.4 ± 12.42 vs. 37.0 ± 11.27 cells/HPF, P = NS, Fig. 4, D and E; vascular
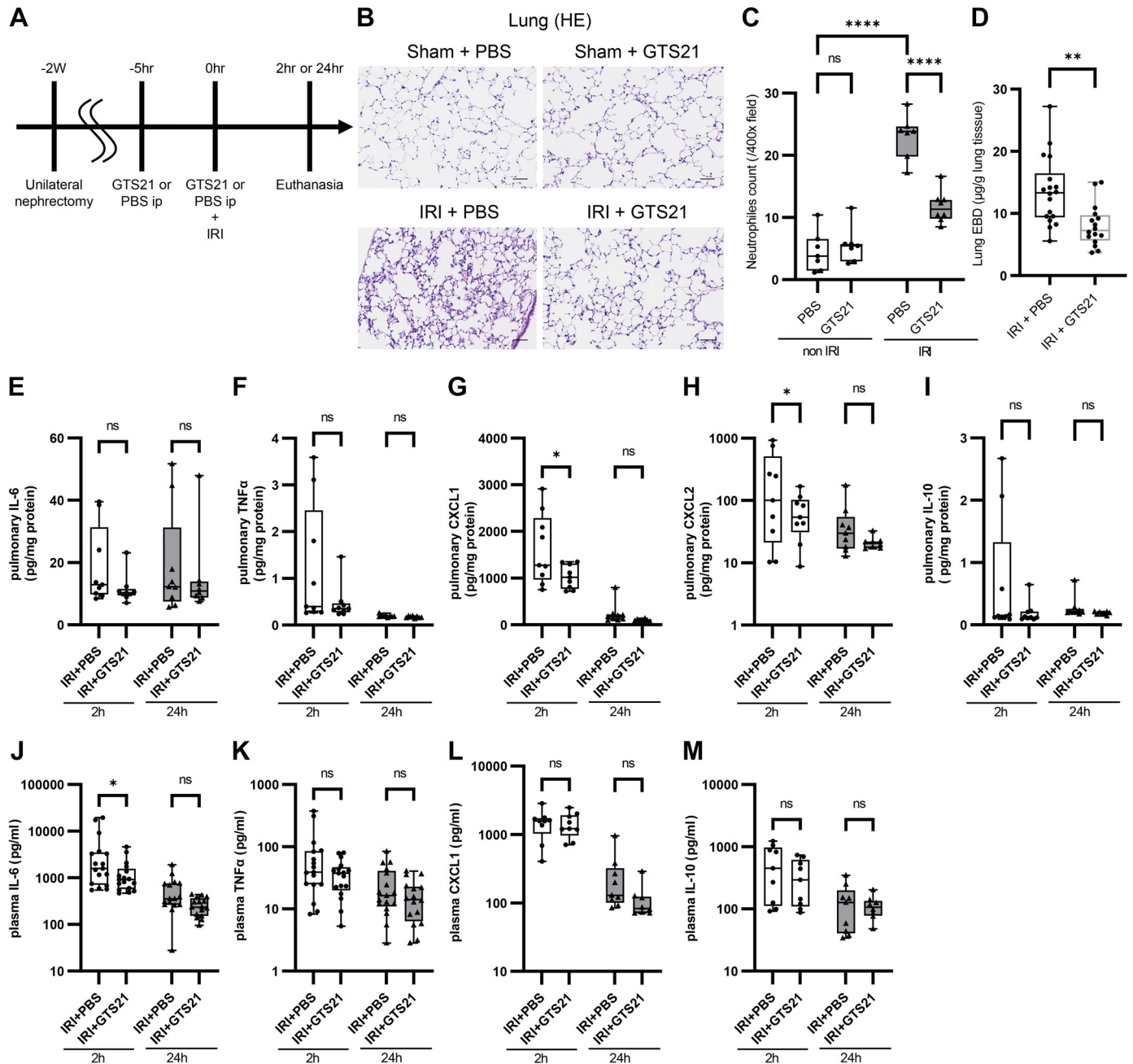
Figure 2. GTS-21 reduced lung neutrophil infiltration 2 h after ischemia-reperfusion injury (IRI), lung Evans blue dye (EBD) leakage 24 h after IRI, and pulmonary chemokine (C-X-C motif) ligand (CXCL)1 and CXCL2 levels 2 h after IRI and plasma IL-6 levels 2 h after IRI. *A*: experiment protocol. *B*: representative images of hematoxylin and eosin (HE)-stained lung tissue. *C*: neutrophil infiltration in the lung 2 h after IRI (*n* = 7 or 8/group). *D*: lung EBD leakage 24 h after IRI (*n* = 16–18/group). *E–I*: pulmonary cytokine levels 2 and 24 h after IRI. *E*: IL-6 (*n* = 8 or 9/group); *F*: TNF-α (*n* = 8 or 9/group); *G*: CXCL1 (*n* = 8 or 9/group); *H*: CXCL2 (*n* = 8 or 9/group); *I*: IL-10 (*n* = 8 or 9/group). *J–M*: plasma cytokine levels 2 and 24 h after IRI. IL-6 (*n* = 16 or 17/group) (*J*), TNF-α (*n* = 16 or 17/group) (*K*), CXCL1 (*n* = 8 or 9/group) (*L*), IL-10 (*n* = 8 or 9/group) (*M*). The data set in *C* was analyzed by two-way ANOVA followed by a Tukey's multiple-comparisons test. The data set in *D* was analyzed by an unpaired *t* test. The other data sets were analyzed by two-way ANOVA followed by Bonferroni's multiple-comparisons tests. The individual data are shown as dots. The *top*, *middle*, and *bottom* lines indicate the 75, 50th, and 25th percentile values, respectively. Whiskers indicate the minimum to maximum values. *$P < 0.05$, **$P < 0.01$, and ****$P < 0.0001$. Scale bars = 50 µm. ns, not significant.

permeability: IRI + GTS-21 vs. IRI + PBS: 49.93 ± 41.770 vs. 34.78 ± 21.550 µg/g lung tissue, $P < 0.01$, Fig. 4F). The necrotic area in the kidney and plasma creatinine significantly increased 24 h after reperfusion (necrotic area: IRI + PBS vs. sham + PBS: 80.7 ± 3.08% vs. 0.2 ± 0.30%, $P < 0.0001$, Supplemental Fig. S5, *A* and *B*; plasma creatinine: IRI + PBS

vs. sham + PBS: 1.71 ± 0.117 vs. 0.18 ± 0.013 mg/dL, $P < 0.0001$, Supplemental Fig. S5C). The administration of GTS-21 slightly decreased the necrotic area in the kidney 24 h after reperfusion (IRI + GTS-21 vs. IRI + PBS: 77.8 ± 2.13% vs. 80.7 ± 3.08%, $P < 0.05$, Supplemental Fig. S5, *A* and *B*). The administration of GTS-21 did not reduce plasma creatinine 24 h after reperfusion
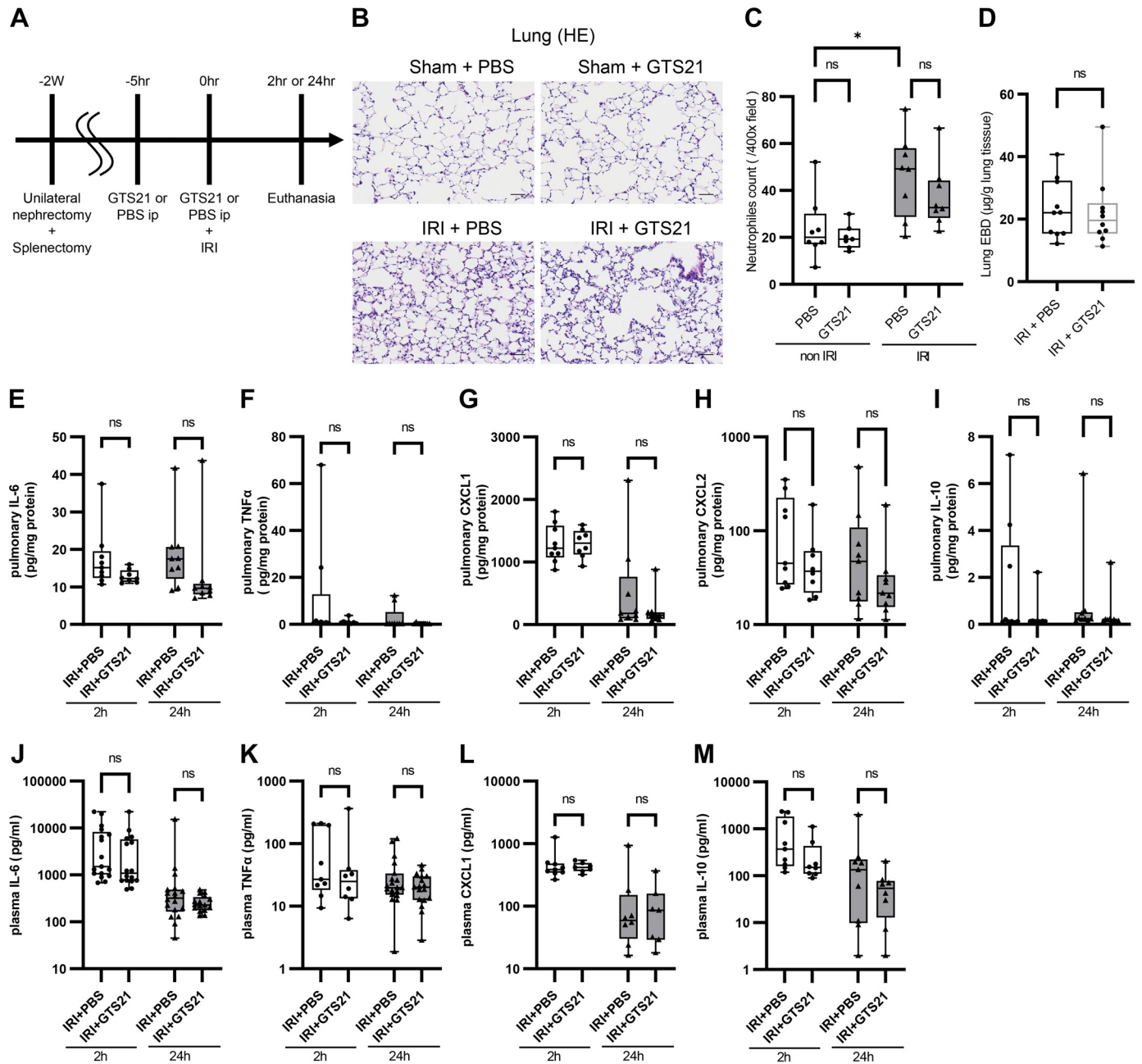
Figure 3. GTS-21 did not reduce lung neutrophil infiltration 2 h after ischemia-reperfusion injury (IRI), lung Evans blue dye (EBD) leakage 24 h after IRI, and pulmonary and plasma cytokine levels 2 and 24 h after IRI in splenectomized mice. *A*: experiment protocol. *B*: representative images of hematoxylin and eosin (HE)-stained lung tissue. *C*: neutrophil infiltration in the lung 2 h after IRI (*n* = 7 or 8/group). *D*: lung EBD leakage 24 h after IRI (*n* = 10/group). *E–I*: pulmonary cytokine levels 2 and 24 h after IRI. IL-6 (*n* = 8 or 9/group) (*E*), TNF-α (*n* = 8 or 9/group) (*F*), chemokine (C-X-C motif) ligand (CXCL)1 (*n* = 8 or 9/group) (*G*), CXCL2 (*n* = 8 or 9/group) (*H*), IL-10 (*n* = 8 or 9/group) (*I*). *J–M*: plasma cytokine levels 2 and 24 h after IRI. IL-6 (*n* = 16–18/group) (*J*), TNF-α (*n* = 9–19/group) (*K*), CXCL1 (*n* = 7–9/group) (*L*), IL-10 (*n* = 8 or 9/group) (*M*). The data set in *C* was analyzed by two-way ANOVA followed by a Tukey's multiple-comparisons test. The data set in *D* was analyzed by unpaired *t* tests. The other data sets were analyzed by two-way ANOVA followed by Bonferroni's multiple-comparisons tests. The individual data are shown as dots. The *top*, *middle*, and *bottom* lines indicate the 75th, 50th, and 25th percentile values, respectively. Whiskers indicate the minimum to maximum values. *$P < 0.05$. Scale bars = 50 μm. ns, not significant.

(IRI + GTS-21 vs. IRI + PBS: 1.70 ± 0.375 vs. 1.71 ± 0.117 mg/dL, *P* = NS, Supplemental Fig. S5*C*).

GTS-21 Reduced Lung Injury After Renal IRI Under Deletion of Alveolar Macrophages

To evaluate whether GTS-21 acts on alveolar macrophages to protect against lung injury after renal IRI, alveolar macrophages were removed intratracheally to give mice 40 μL/day of clodronate liposomes 3 days before IRI (Fig. 5*A*). In mice treated by intratracheal administration of clodronate liposomes, red pulp macrophages in the spleen did not change (clodronate vs. control: 1.34 ± 0.329 vs. 1.24 ± 0.150 × 10^6 cells/whole spleen, *P* = NS, Fig. 5*B*), but alveolar macrophages were significantly reduced
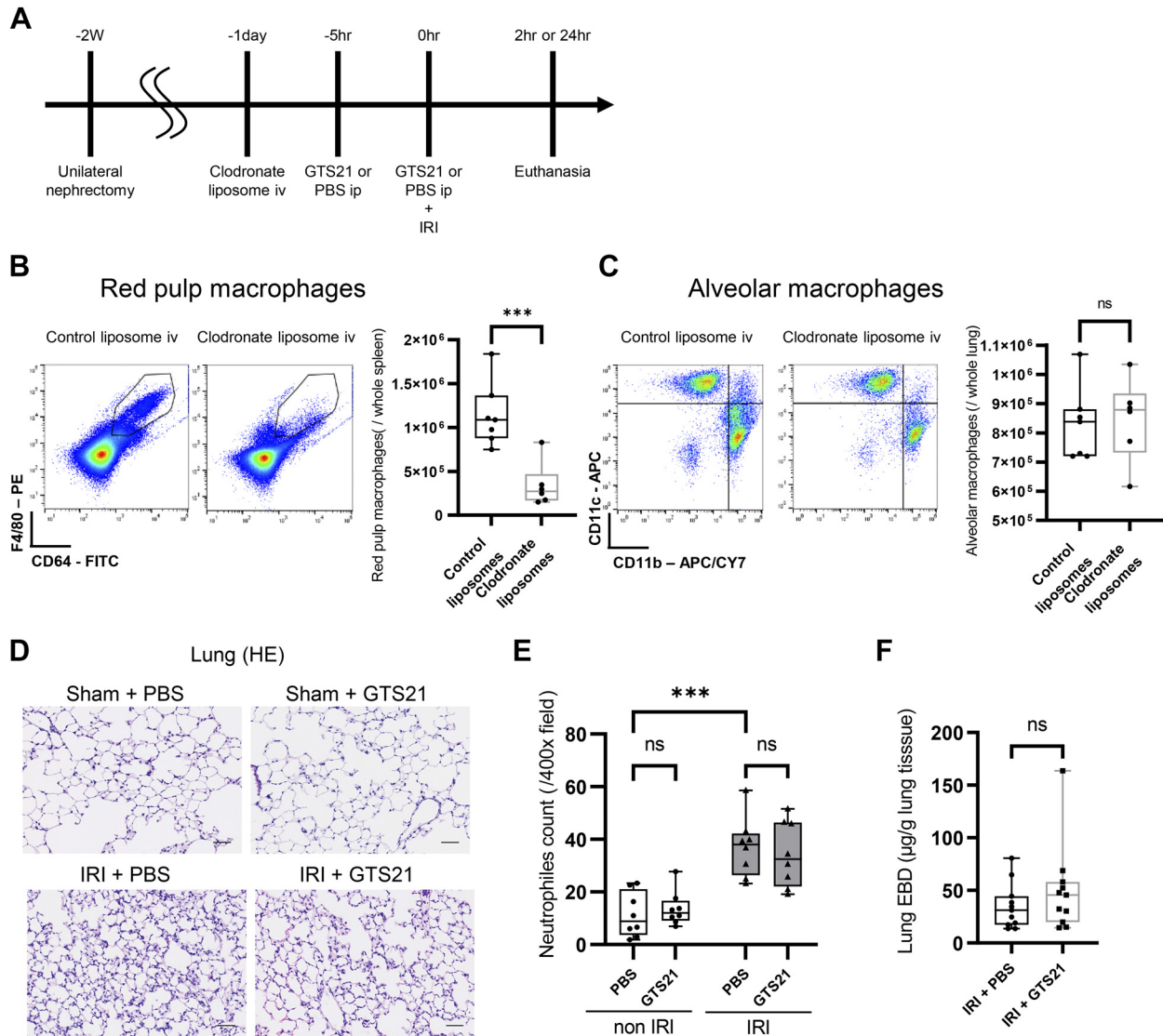
Figure 4. GTS-21 did not reduce lung neutrophil infiltration 2 h after ischemia-reperfusion injury (IRI) and lung Evans blue dye (EBD) leakage 24 h after IRI in mice whose splenic macrophages and systemic mononuclear phagocytes were deleted. *A*: experiment protocol. *B*: red pulp macrophages calculated by flow cytometry (*n* = 6 or 7/group). *C*: alveolar macrophages calculated by flow cytometry (*n* = 6 or 7/group). *D*: representative images of hematoxylin and eosin (HE)-stained lung tissue. *E*: neutrophil infiltration in the lung 2 h after IRI (*n* = 8/group). *F*: lung EBD leakage 24 h after IRI (*n* = 11/group). The data set in *F* was analyzed by two-way ANOVA followed by a Tukey's multiple-comparisons test. The other data sets were analyzed by unpaired *t* tests. The individual data are shown as dots. The *top*, *middle*, and *bottom* lines indicate the 75th, 50th, and 25th percentile values, respectively. Whiskers indicate the minimum to maximum values. ***$P < 0.001$. Scale bars = 50 μm. ns, not significant.

(clodronate vs. control: $3.01 ± 0.547$ vs. $5.29 ± 1.144 × 10^5$ cells/whole lung, $P < 0.05$, Fig. 5*C*). The lungs were heavily infiltrated with neutrophils 2 h after renal IRI (IRI + PBS vs. sham + PBS: $21.0 ± 8.05$ vs. $5.1 ± 1.77$ cells/HPF, $P < 0.001$, Fig. 5, *D* and *E*). In contrast to mice treated with intravenous administration of clodronate liposomes, in mice treated by intratracheal administration of clodronate liposomes, GTS-21 significantly reduced lung neutrophil infiltration at 2 h and vascular permeability at 24 h after reperfusion (neutrophil infiltration: IRI + GTS-21 vs. IRI + PBS: $12.9 ± 3.89$ vs. $21.0 ± 8.05$ cells/HPF, $P < 0.05$, Fig. 5, *D* and *E*; vascular permeability: IRI + GTS-21 vs. IRI + PBS: $9.74 ± 2.361$ vs. $13.86 ± 4.789$ μg/g lung tissue, $P < 0.05$, Fig. 5*F*).The necrotic area in the kidney and plasma creatinine increased 24 h after reperfusion (necrotic area: IRI +

PBS vs. sham + PBS: $78.8 ± 2.61\%$ vs. $0.1 ± 0.14\%$, $P < 0.0001$, Supplemental Fig. S6, *A* and *B*; plasma creatinine: IRI + PBS vs. sham + PBS: $1.98 ± 0.169$ vs. $0.17 ± 0.014$ mg/dL, $P < 0.0001$, Supplemental Fig. S6*C*). The administration of GTS-21 did not reduce the necrotic area in the kidney and plasma creatinine 24 h after reperfusion (necrotic area: IRI + GTS-21 vs. IRI + PBS: $76.5 ± 3.21\%$ vs. $78.8 ± 2.61\%$, $P = $ NS, Supplemental Fig. S6, *A* and *B*; plasma creatinine: IRI + GTS-21 vs. IRI + PBS: $1.85 ± 0.093$ vs. $1.98 ± 0.169$ mg/dL, $P = $ NS, Supplemental Fig. S6*C*).

DISCUSSION

This study showed, for the first time, the beneficial effect of nAChR agonists on ALI after AKI due to renal IRI. The
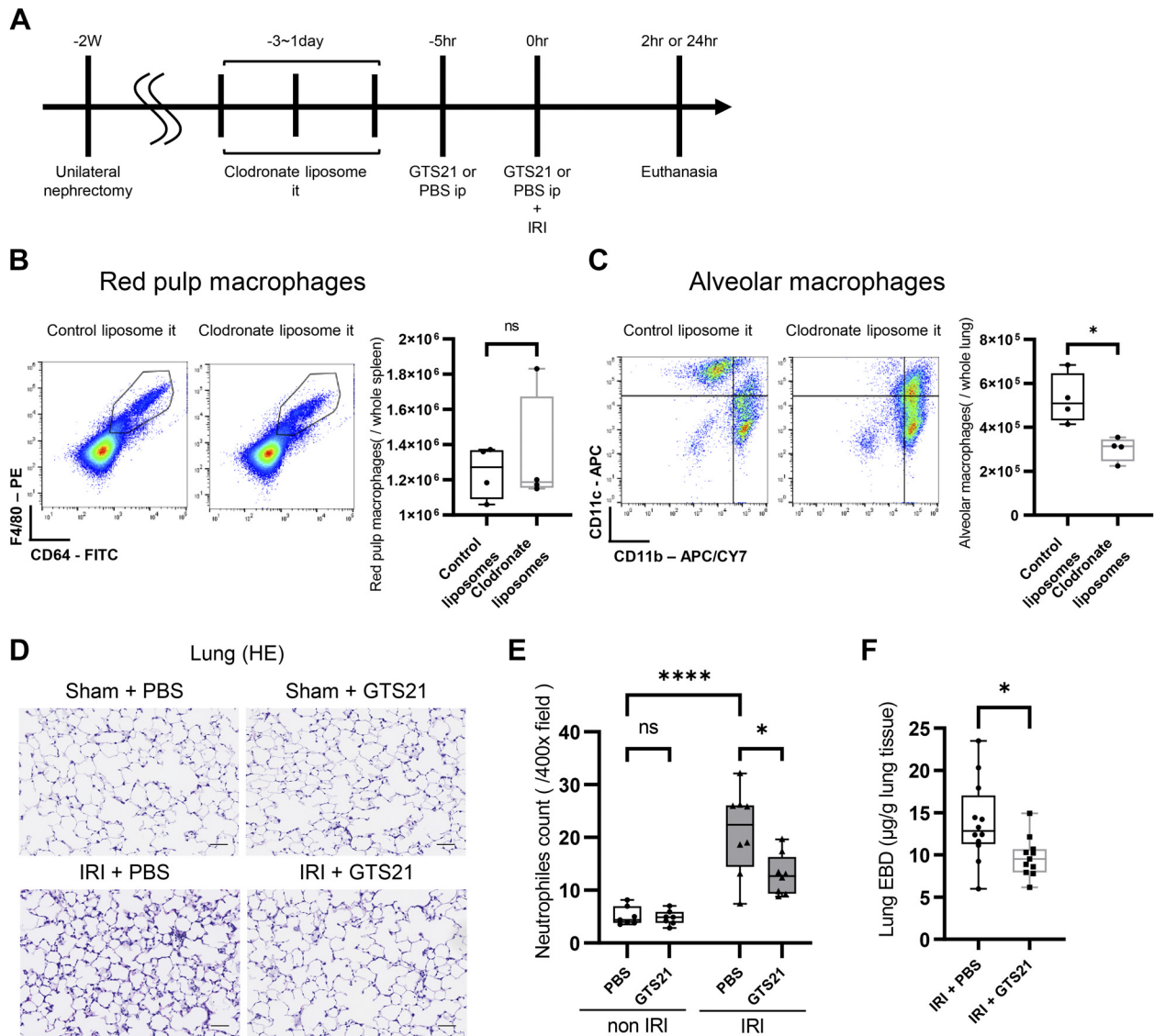
Figure 5. GTS-21 reduced lung neutrophil infiltration 2 h after ischemia-reperfusion injury (IRI) and lung Evans blue dye (EBD) leakage 24 h after IRI in mice whose alveolar macrophages were deleted. *A*: experiment protocol. *B*: red pulp macrophages calculated by flow cytometry (*n* = 4/group). *C*: alveolar macrophages calculated by flow cytometry (*n* = 4/group). *D*: representative images of hematoxylin and eosin (HE)-stained lung tissue. *E*: neutrophil infiltration in the lung 2 h after IRI (*n* = 7 or 8/group). *F*: lung EBD leakage 24 h after IRI (*n* = 11 or 12/group). The data sets in *B* and *C* were analyzed by Mann–Whitney tests. The data set in *E* was analyzed by two-way ANOVA followed by a Tukey's multiple-comparisons test. The data set in *F* was analyzed by an unpaired *t* test. The individual data are shown as dots. The *top*, *middle*, and *bottom* lines indicate the 75th, 50th, and 25th percentile values, respectively. Whiskers indicate the minimum to maximum values. *$P < 0.05$ and ****$P < 0.0001$. Scale bars = 50 μm. ns, not significant.

findings are summarized as follows: *1*) nAChR agonists reduced lung neutrophil infiltration and vascular permeability and upregulated pulmonary CXCL1, CXCL2, and plasma IL-6 levels after renal IRI; *2*) the effect of GTS-21, a selective α7nAChR agonist, on plasma IL-6 and lungs was eliminated in splenectomized mice; *3*) the effect of GTS-21 on the lungs was diminished in mice depleted of splenic macrophages and systemic mononuclear phagocytes; and *4*) the effect of GTS-21 on the lungs was not diminished in mice with depleted alveolar macrophages. These findings suggest that nAChR agonist reduces ALI after IRI-induced AKI via macrophages in the spleen.

Nicotine reduced neutrophil infiltration and vascular permeability in the lungs after renal IRI. Neutrophil infiltration,

vascular permeability, and CXCL1 and CXCL2 levels in the lung after renal IRI were reduced by GTS-21. An official American Thoracic Society workshop ([31]) reported that three of four features—*1*) histological evidence of tissue injury, *2*) alteration of the alveolar capillary barrier, *3*) an inflammatory response, and *4*) evidence of physiological dysfunction —should be shown in experimental ALI models. Evidence of tissue injury includes accumulation of neutrophils as a very relevant marker. Evidence of the inflammatory response includes proinflammatory cytokines in lung tissue. In this study, lung neutrophil counts representing histological tissue injury, EBD staining representing vascular permeability, and lung CXCL1 level representing the inflammatory response were evaluated as injury markers of ALI. These

assessments met the criteria for the evaluation of ALI in animal experiments. These results indicate that nAChR agonists attenuate lung injury induced by AKI. Our findings were consistent with those of previous reports showing the beneficial effects of nAChR agonists on noninfectious lung injury models, such as administration of acid or LPS and hyperoxia (40–43). In infectious models, the effects of nAChR agonists on lung injury are mostly consistent. Although nAChR agonists improve acute *Escherichia coli* pneumonia (44), nAChR agonists exacerbate acute lung injury by polymicrobial peritonitis and pneumococcal pneumonia by impairing host defense (45, 46). Thus, nAChR agonists could protect against ALI in noninfectious and infectious states if the infection is under control. Administration of nAChR agonists had little effect on the renal necrotic area, and plasma creatinine increased after renal IRI. These results suggest that the protective effects of AChR agonists on lung injury were not due to the improvement of kidney injury induced by AChR agonists. In contrast to our results, Yeboah et al. (28) reported that the administration of nAChR agonists improved renal damage caused by renal IRI, and Inoue et al. (47) reported that VNS improved renal damage caused by IRI via splenic α7nACR activation. These differences could be attributed to differences in the severity of kidney injury and the timing of AChR activation. In particular, our renal IRI model caused severe damage, with 80% of the OSOM being necrotic, that could not be alleviated by AChR agonists.

We evaluated the sites of anti-inflammatory action of GTS-21 after renal IRI. With the administration of GTS-21, there was no reduction in neutrophil infiltration, vascular permeability, and CXCL1 and CXCL2 levels in the lungs after renal IRI in splenectomized mice and mice depleted of splenic macrophages and systemic mononuclear phagocytes by intravenous injection of clodronate liposomes. These findings indicate that the action of the nAChR agonist on the spleen, especially splenic macrophages, contributed to the attenuation of ALI after AKI. These mechanisms of action of GTS-21 participate in the CAP (48). Activation of the catecholaminergic splenic nerve releases norepinephrine from its terminals, which interacts with choline acetyltransferase-positive T-cells in the spleen, causing ACh release; ACh binds to α7nAChRs expressed on macrophages, resulting in the suppression of proinflammatory cytokine production, such as TNF-α and IL-6 (20, 23, 24). Thus, in the CAP concept, the spleen could be treated as a proinflammatory organ. This evidence suggests that in the remote action of AKI in lung injury, the spleen is an important immunomodulatory transit point and could act as a proinflammatory organ and that GTS-21 reduces ALI via the splenic CAP. However, it has been reported that the spleen is an important organ that exerts anti-inflammatory actions in the model of ALI (18, 49, 50). Andres-Hernando et al. (18, 50) reported that splenectomy upregulated circulating IL-6 and exacerbated lung injury after renal IRI and that IL-10 in splenic $CD4^+$ T-cells upregulated by IL-6 limited lung inflammation after renal IRI. The spleen has the ability to produce IL-10, which antagonizes IL-6. IL-6 causes lung injury by increasing CXCL1 production, neutrophil infiltration, and vascular permeability via action on pulmonary endothelial cells (15, 16, 51, 52). Our finding that GTS-21 reduced circulating IL-6 levels in mice with spleens but

not in splenectomized mice suggests that circulating IL-6 is reduced via the spleen by GTS-21. It appears reasonable that GTS-21 could suppress IL-6 production in splenic macrophages after AKI, because GTS-21 reduced IL-6 and TNF-α production by macrophages in vitro (53). However, IL-6 has been shown to be produced by the kidney and liver as well as the spleen after renal IRI (18, 54). In splenectomized mice, IL-6 may be produced by the liver and kidneys in a compensatory manner to escape the anti-inflammatory effect of the spleen after AKI, resulting in lung injury. This hypothesis has not been tested (18), and further studies are needed to evaluate it. GTS-21 might indirectly decrease IL-6 production in the liver and kidneys via the splenic CAP. GTS-21 did not alter circulating IL-10 level after AKI with or without the spleen, suggesting that circulating IL-10 had little effect on the effect of GTS-21 in reducing lung injury after AKI. Thus, GTS-21 exerted its anti-inflammatory effect by suppressing the production of proinflammatory circulating IL-6 rather than enhancing the production of the anti-inflammatory cytokine IL-10 via splenic macrophages.

We evaluated another site, alveolar macrophages, of the anti-inflammatory action of GTS-21 after renal IRI. In mice intratracheally administered clodronate liposomes, GTS-21 reduced the infiltration of neutrophils and vascular permeability in the lung after renal IRI. These findings indicate that alveolar macrophages were not involved in the protective effects of the nAChR agonist on ALI after AKI. Although alveolar macrophages have been shown to be involved in lung injuries such as infection, ventilator induced, and instillation of endotoxin (55–59), the role of alveolar macrophages in ALI after renal IRI has been reported as follows: the intratracheal administration of clodronate liposomes diminished lung capillary leak and exacerbated lung CXCL1 and myeloperoxidase activity after bilateral renal IRI (14). The major reason for GTS-21 not acting on alveolar macrophages despite the previous report of the effects of alveolar macrophages after AKI might be attributed to the anatomy. Alveolar macrophages are present in the alveolar space and are in contact with antigens in the respiratory tract, causing an immune response without exposure to blood. Cytokines, including IL-6 and damage-associated molecular patterns released into the blood circulation after AKI, might expose less alveolar macrophages to act on than circulating monocytes and/or splenic macrophages. In fact, intravenous administration of clodronate liposomes reduced intrasplenic macrophages but did not affect alveolar macrophages. Thus, alveolar macrophages act against direct injury from the airways but have less effect on lung injury due to remote effects from AKI, and the anti-inflammatory effect of GTS-21 on alveolar macrophages may not have been sufficient to protect against lung injury. There could be functional differences between alveolar and splenic macrophages. Splenic macrophages express more Toll-like receptor (TLR)9 than alveolar macrophages and migrate to the lungs via the function of CpG motif-rich DNA, a ligand for TLR9. Alveolar macrophages have high expression levels of TLR4 instead of TLR9 and proliferate under stimulation by LPS, a ligand for TLR4. In renal IRI, damage-associated pathogens, including mitochondrial DNA, are released from the kidney (16). Although we did not evaluate the role of interstitial macrophages in ALI after AKI, interstitial macrophages derived from the

spleen might have more effects on lung injury after AKI than resident alveolar macrophages. Sabatel et al. (60) reported that intrasplenic monocytes migrate into the alveolar interstitium and protect against asthma when CpG motif-rich oligodeoxynucleotides were administered, suggesting that interstitial macrophages primed by GTS-21, originating from the spleen, might act against lung injury. Further studies are needed to clarify the detailed mechanisms of action of pulmonary macrophages in ALI after AKI. We will conduct further studies, including those involving reconstitution, to elucidate the differences between spleen and lung macrophages in the pathogenesis of ALI induced by AKI.

This study has some limitations. First, only lung EBD staining was used for evaluating extravascular lung water, although there are other markers such as the lung wet-to-dry ratio and bronchoalveolar lavage protein. Our model was that of an indirect lung injury by systemic response after AKI, making it difficult to find suitable methods to evaluate the wet-to-dry ratio and bronchoalveolar lavage protein concentration. In this study, lung neutrophil count representing histological tissue injury, EBD staining representing vascular permeability, and lung CXCL1 levels representing the inflammatory response were evaluated as injury markers of experimental ALI. These assessments met the criteria for the evaluation of ALI in animal experiments (31). Second, intravenous administration of clodronate liposomes has systemic effects and affects not only splenic macrophages but also Kupffer cells of the liver and circulating monocytes (61). Based on results with two experimental settings of splenectomy and intravenous administration of clodronate liposomes, the site of action of nAChR agonist was shown to be splenic macrophages. Third, in the model of deletion of alveolar macrophage by intratracheal instillation of clodronate liposomes, a certain amount of alveolar macrophages remained. The remaining alveolar macrophages may confound the effect of GTS-21. However, the disappearance of the pulmonary protective effect of GTS-21 despite a certain amount of red pulp macrophages remaining by intravenous administration of clodronate indicates that the reduction in the alveolar macrophage count by intratracheal administration of clodronate was sufficient. Fourth, the baseline levels of lung injury varied among experimental settings. The experimental setting without the spleen or without splenic macrophages tended to have higher lung neutrophil counts and lung EBD values in mice with sham operation than the experimental settings with the spleen (Fig. 1, C and D, Fig. 2, C and D, Fig. 3, C and D, Fig. 4, E and F, and Fig. 5, E and F). Although it was difficult to compare different experimental settings, the increase in the levels of lung injury markers in mice with sham operation might be caused by splenectomy or splenic macrophage depletion. Our results are consistent with those in a previous report that suggest that splenectomy exacerbates lung damage caused by AKI (18).

Perspectives and Significance

We demonstrated, for the first time, that nAChR agonists reduced lung injury induced by AKI even though they did not ameliorate renal injury. The action mechanism of nAChR agonists on ALI involved anti-inflammatory effects on splenic, but not alveolar, macrophages with subsequent downregulation of circulating IL-6. nAChR agonists have the potential to break the organ-organ cross-talk from AKI to ALI via splenic macrophages.

DISCLOSURES

No conflicts of interest, financial or otherwise, are declared by the authors.

AUTHOR CONTRIBUTIONS

D.G. and H.Y. conceived and designed research; D.G., S.N., and Y.N. performed experiments; D.G., S.N., Y.N., and H.Y. analyzed data; D.G., S.I., T.I., T.F., N.O., and H.Y. interpreted results of experiments; D.G. and H.Y. prepared figures; D.G. and H.Y. drafted manuscript; H.Y. edited and revised manuscript; D.G., S.N., Y.N., S.I., T.I., T.F., N.O., A.K., H.M., K.S., and H.Y. approved final version of manuscript.

REFERENCES

1. **Al-Jaghbeer M, Dealmeida D, Bilderback A, Ambrosino R, Kellum JA.** Clinical decision support for in-hospital AKI. *J Am Soc Nephrol* 29: 654–660, 2018. doi:10.1681/ASN.2017070765.

2. **Hoste EA, Bagshaw SM, Bellomo R, Cely CM, Colman R, Cruz DN, Edipidis K, Forni LG, Gomersall CD, Govil D, Honoré PM, Joannes-Boyau O, Joannidis M, Korhonen AM, Lavrentieva A, Mehta RL, Palevsky P, Roessler E, Ronco C, Uchino S, Vazquez JA, Vidal Andrade E, Webb S, Kellum JA.** Epidemiology of acute kidney injury in critically ill patients: the multinational AKI-EPI study. *Intensive Care Med* 41: 1411–1423, 2015. doi:10.1007/s00134-015-3934-7.

3. **Chertow GM, Burdick E, Honour M, Bonventre JV, Bates DW.** Acute kidney injury, mortality, length of stay, and costs in hospitalized patients. *J Am Soc Nephrol* 16: 3365–3370, 2005. doi:10.1681/ASN.2004090740.

4. **Wang Y, Gallagher M, Li Q, Lo S, Cass A, Finfer S, Myburgh J, Bouman C, Faulhaber-Walter R, Kellum JA, Palevsky PM, Ronco C, Saudan P, Tolwani A, Bellomo R.** Renal replacement therapy intensity for acute kidney injury and recovery to dialysis independence: a systematic review and individual patient data meta-analysis. *Nephrol Dial Transplant* 33: 1017–1024, 2018. doi:10.1093/ndt/gfx308.

5. **Gaudry S, Hajage D, Benichou N, Chaïbi K, Barbar S, Zarbock A, Lumlertgul N, Wald R, Bagshaw SM, Srisawat N, Combes A, Geri G, Jamale T, Dechartres A, Quenot J-P, Dreyfuss D.** Delayed versus early initiation of renal replacement therapy for severe acute kidney injury: a systematic review and individual patient data meta-analysis of randomised clinical trials. *Lancet* 395: 1506–1515, 2020. doi:10.1016/S0140-6736(20)30531-6.

6. **Doi K**, **Rabb H.** Impact of acute kidney injury on distant organ function: recent findings and potential therapeutic targets. *Kidney Int* 89: 555–564, 2016. doi:10.1016/j.kint.2015.11.019.

7. **Yasuda H**, **Kato A**, **Fujigaki Y**, **Hishida A**; **Shizuoka Kidney Disease Study Group.** Incidence and clinical outcomes of acute kidney injury requiring renal replacement therapy in Japan. *Ther Apher Dial* 14: 541–546, 2010. doi:10.1111/j.1744-9987.2010.00826.x.

8. **Chertow GM**, **Christiansen CL**, **Cleary PD**, **Munro C**, **Lazarus JM.** Prognostic stratification in critically ill patients with acute renal failure requiring dialysis. *Arch Intern Med* 155: 1505–1511, 1995.

9. **Chao CT**, **Hou CC**, **Wu VC**, **Lu HM**, **Wang CY**, **Chen L**, **Kao TW.** The impact of dialysis-requiring acute kidney injury on long-term prognosis of patients requiring prolonged mechanical ventilation: nationwide population-based study. *PLoS One* 7: e50675, 2012. doi:10.1371/journal.pone.0050675.

10. **Demirjian S**, **Chertow GM**, **Zhang JH**, **O'Connor TZ**, **Vitale J**, **Paganini EP**, **Palevsky PM**; **VA/NIH Acute Renal Failure Trial Network.** Model to predict mortality in critically ill adults with acute kidney injury. *Clin J Am Soc Nephrol* 6: 2114–2120, 2011. doi:10.2215/CJN.02900311.

11. **Vieira JM Jr**, **Castro I**, **Curvello-Neto A**, **Demarzo S**, **Caruso P**, **Pastore L Jr**, **Imanishe MH**, **Abdulkader RC**, **Deheinzelin D.** Effect of acute kidney injury on weaning from mechanical ventilation in critically ill patients. *Crit Care Med* 35: 184–191, 2007. doi:10.1097/01.CCM.0000249828.81705.65.

12. **Wald R**, **McArthur E**, **Adhikari NK**, **Bagshaw SM**, **Burns KE**, **Garg AX**, **Harel Z**, **Kitchlu A**, **Mazer CD**, **Nash DM**, **Scales DC**, **Silver SA**, **Ray JG**, **Friedrich JO.** Changing incidence and outcomes following dialysis-requiring acute kidney injury among critically ill adults: a population-based cohort study. *Am J Kidney Dis* 65: 870–877, 2015. doi:10.1053/j.ajkd.2014.10.017.

13. **Lee SA**, **Cozzi M**, **Bush EL**, **Rabb H.** Distant organ dysfunction in acute kidney injury: a review. *Am J Kidney Dis* 72: 846–856, 2018. doi:10.1053/j.ajkd.2018.03.028.

14. **Altmann C**, **Andres-Hernando A**, **McMahan RH**, **Ahuja N**, **He Z**, **Rivard CJ**, **Edelstein CL**, **Barthel L**, **Janssen WJ**, **Faubel S.** Macrophages mediate lung inflammation in a mouse model of ischemic acute kidney injury. *Am J Physiol Renal Physiol* 302: F421–F432, 2012. doi:10.1152/ajprenal.00559.2010.

15. **Ahuja N**, **Andres-Hernando A**, **Altmann C**, **Bhargava R**, **Bacalja J**, **Webb RG**, **He Z**, **Edelstein CL**, **Faubel S.** Circulating IL-6 mediates lung injury via CXCL1 production after acute kidney injury in mice. *Am J Physiol Renal Physiol* 303: F864–F872, 2012. doi:10.1152/ajprenal.00025.2012.

16. **Faubel S**, **Edelstein CL.** Mechanisms and mediators of lung injury after acute kidney injury. *Nat Rev Nephrol* 12: 48–60, 2016. doi:10.1038/nrneph.2015.158.

17. **Skrypnyk NI**, **Gist KM**, **Okamura K**, **Montford JR**, **You Z**, **Yang H**, **Moldovan R**, **Bodoni E**, **Blaine JT**, **Edelstein CL**, **Soranno DE**, **Kirkbride-Romeo LA**, **Griffin BR**, **Altmann C**, **Faubel S.** IL-6-mediated hepatocyte production is the primary source of plasma and urine neutrophil gelatinase-associated lipocalin during acute kidney injury. *Kidney Int* 97: 966–979, 2020. doi:10.1016/j.kint.2019.11.013.

18. **Andrés-Hernando A**, **Altmann C**, **Ahuja N**, **Lanaspa MA**, **Nemenoff R**, **He Z**, **Ishimoto T**, **Simpson PA**, **Weiser-Evans MC**, **Bacalja J**, **Faubel S.** Splenectomy exacerbates lung injury after ischemic acute kidney injury in mice. *Am J Physiol Renal Physiol* 301: F907–F916, 2011. doi:10.1152/ajprenal.00107.2011.

19. **Kramer AA**, **Postler G**, **Salhab KF**, **Mendez C**, **Carey LC**, **Rabb H.** Renal ischemia/reperfusion leads to macrophage-mediated increase in pulmonary vascular permeability. *Kidney Int* 55: 2362–2367, 1999. doi:10.1046/j.1523-1755.1999.00460.x.

20. **Wang H**, **Yu M**, **Ochani M**, **Amella CA**, **Tanovic M**, **Susarla S**, **Li JH**, **Wang H**, **Yang H**, **Ulloa L**, **Al-Abed Y**, **Czura CJ**, **Tracey KJ.** Nicotinic acetylcholine receptor α7 subunit is an essential regulator of inflammation. *Nature* 421: 384–388, 2003. doi:10.1038/nature01339.

21. **Pavlov VA**, **Ochani M**, **Yang LH**, **Gallowitsch-Puerta M**, **Ochani K**, **Lin X**, **Levi J**, **Parrish WR**, **Rosas-Ballina M**, **Czura CJ**, **Larosa GJ**, **Miller EJ**, **Tracey KJ**, **Al-Abed Y.** Selective α7-nicotinic acetylcholine receptor agonist GTS-21 improves survival in murine endotoxemia and severe sepsis. *Crit Care Med* 35: 1139–1144, 2007. doi:10.1097/01.CCM.0000259381.56526.96.

22. **Huston JM**, **Ochani M**, **Rosas-Ballina M**, **Liao H**, **Ochani K**, **Pavlov VA**, **Gallowitsch-Puerta M**, **Ashok M**, **Czura CJ**, **Foxwell B**, **Tracey KJ**, **Ulloa L.** Splenectomy inactivates the cholinergic antiinflammatory pathway during lethal endotoxemia and polymicrobial sepsis. *J Exp Med* 203: 1623–1628, 2006. doi:10.1084/jem.20052362.

23. **Rosas-Ballina M**, **Olofsson PS**, **Ochani M**, **Valdés-Ferrer SI**, **Levine YA**, **Reardon C**, **Tusche MW**, **Pavlov VA**, **Andersson U**, **Chavan S**, **Mak TW**, **Tracey KJ.** Acetylcholine-synthesizing T cells relay neural signals in a vagus nerve circuit. *Science* 334: 98–101, 2011. doi:10.1126/science.1209985.

24. **Rosas-Ballina M**, **Ochani M**, **Parrish WR**, **Ochani K**, **Harris YT**, **Huston JM**, **Chavan S**, **Tracey KJ.** Splenic nerve is required for cholinergic antiinflammatory pathway control of TNF in endotoxemia. *Proc Natl Acad Sci USA* 105: 11008–11013, 2008. doi:10.1073/pnas.0803237105.

25. **Kox M**, **Vaneker M**, **van der Hoeven JG**, **Scheffer GJ**, **Hoedemaekers CW**, **Pickkers P.** Effects of vagus nerve stimulation and vagotomy on systemic and pulmonary inflammation in a two-hit model in rats. *PLoS One* 7: e34431, 2012. doi:10.1371/journal.pone.0034431.

26. **Galvis G**, **Lips KS**, **Kummer W.** Expression of nicotinic acetylcholine receptors on murine alveolar macrophages. *J Mol Neurosci* 30: 107–108, 2006. doi:10.1385/JMN:30:1:107.

27. **Wang J**, **Li R**, **Peng Z**, **Zhou W**, **Hu B**, **Rao X**, **Yang X**, **Li J.** GTS-21 reduces inflammation in acute lung injury by regulating M1 polarization and function of alveolar macrophages. *Shock* 51: 389–400, 2019. doi:10.1097/SHK.0000000000001144.

28. **Yeboah MM**, **Xue X**, **Duan B**, **Ochani M**, **Tracey KJ**, **Susin M**, **Metz CN.** Cholinergic agonists attenuate renal ischemia-reperfusion injury in rats. *Kidney Int* 74: 62–69, 2008. doi:10.1038/ki.2008.94.

29. **Hoke TS**, **Douglas IS**, **Klein CL**, **He Z**, **Fang W**, **Thurman JM**, **Tao Y**, **Dursun B**, **Voelkel NF**, **Edelstein CL**, **Faubel S.** Acute renal failure after bilateral nephrectomy is associated with cytokine-mediated pulmonary injury. *J Am Soc Nephrol* 18: 155–164, 2007. doi:10.1681/ASN.2006050494.

30. **Marschner JA**, **Schäfer H**, **Holderied A**, **Anders HJ.** Optimizing mouse surgery with online rectal temperature monitoring and preoperative heat supply. Effects on post-ischemic acute kidney injury. *PLoS One* 11: e0149489, 2016. doi:10.1371/journal.pone.0149489.

31. **Matute-Bello G**, **Downey G**, **Moore BB**, **Groshong SD**, **Matthay MA**, **Slutsky AS**, **Kuebler WM**; **Acute Lung Injury in Animals Study Group.** An official American Thoracic Society workshop report: features and measurements of experimental acute lung injury in animals. *Am J Respir Cell Mol Biol* 44: 725–738, 2011. doi:10.1165/rcmb.2009-0210ST.

32. **Wang le F**, **Patel M**, **Razavi HM**, **Weicker S**, **Joseph MG**, **McCormack DG**, **Mehta S.** Role of inducible nitric oxide synthase in pulmonary microvascular protein leak in murine sepsis. *Am J Respir Crit Care Med* 165: 1634–1639, 2002. doi:10.1164/rccm.2110017.

33. **Nabe T**, **Matsuda M**, **Ishida T**, **Tsujimoto N**, **Kido H**, **Kanaya H**, **Takahashi H**, **Takemoto N**, **Nomura M**, **Ishihara K**, **Akiba S**, **Mizutani N.** Antigen-specific airway IL-33 production depends on FcγR-mediated incorporation of the antigen by alveolar macrophages in sensitized mice. *Immunology* 155: 99–111, 2018. doi:10.1111/imm.12931.

34. **Guilliams M**, **Dutertre CA**, **Scott CL**, **McGovern N**, **Sichien D**, **Chakarov S**, **Van Gassen S**, **Chen J**, **Poidinger M**, **De Prijck S**, **Tavernier SJ**, **Low I**, **Irac SE**, **Mattar CN**, **Sumatoh HR**, **Low GHL**, **Chung TJK**, **Chan DKH**, **Tan KK**, **Hon TLK**, **Fossum E**, **Bogen B**, **Choolani M**, **Chan JKY**, **Larbi A**, **Luche H**, **Henri S**, **Saeys Y**, **Newell EW**, **Lambrecht BN**, **Malissen B**, **Ginhoux F.** Unsupervised high-dimensional analysis aligns dendritic cells across tissues and species. *Immunity* 45: 669–684, 2016. doi:10.1016/j.immuni.2016.08.015.

35. **Zaynagetdinov R**, **Sherrill TP**, **Kendall PL**, **Segal BH**, **Weller KP**, **Tighe RM**, **Blackwell TS.** Identification of myeloid cell subsets in murine lungs using flow cytometry. *Am J Respir Cell Mol Biol* 49: 180–189, 2013. doi:10.1165/rcmb.2012-0366MA.

36. **Zoli M**, **Pucci S**, **Vilella A**, **Gotti C.** Neuronal and extraneuronal nicotinic acetylcholine receptors. *Curr Neuropharmacol* 16: 338–349, 2018. doi:10.2174/1570159X15666170912110450.

37. **Krais AM**, **Hautefeuille AH**, **Cros MP**, **Krutovskikh V**, **Tournier JM**, **Birembaut P**, **Thépot A**, **Paliwal A**, **Herceg Z**, **Boffetta P**, **Brennan P**, **Hainaut PL.** CHRNA5 as negative regulator of nicotine signaling in normal and cancer bronchial cells: effects on motility, migration and p63 expression. *Carcinogenesis* 32: 1388–1395, 2011. doi:10.1093/carcin/bgr090.

38. **Fujiyama S**, **Nakahashi-Oda C**, **Abe F**, **Wang Y**, **Sato K**, **Shibuya A.** Identification and isolation of splenic tissue-resident macrophage sub-populations by flow cytometry. *Int Immunol* 31: 51–56, 2019. doi:10.1093/intimm/dxy064.

39. **A-Gonzalez N**, **Guillen JA**, **Gallardo G**, **Diaz M**, **de la Rosa JV**, **Hernandez IH**, **Casanova-Acebes M**, **Lopez F**, **Tabraue C**, **Beceiro S**, **Hong C**, **Lara PC**, **Andujar M**, **Arai S**, **Miyazaki T**, **Li S**, **Corbi AL**, **Tontonoz P**, **Hidalgo A**, **Castrillo A.** The nuclear receptor LXRα controls the functional specialization of splenic macrophages. *Nat Immunol* 14: 831–839, 2013. doi:10.1038/ni.2622.

40. **Su X**, **Lee JW**, **Matthay ZA**, **Mednick G**, **Uchida T**, **Fang X**, **Gupta N**, **Matthay MA.** Activation of the α7 nAChR reduces acid-induced acute lung injury in mice and rats. *Am J Respir Cell Mol Biol* 37: 186–192, 2007. doi:10.1165/rcmb.2006-0240OC.

41. **Ni YF**, **Tian F**, **Lu ZF**, **Yang GD**, **Fu HY**, **Wang J**, **Yan XL**, **Zhao YC**, **Wang YJ**, **Jiang T.** Protective effect of nicotine on lipopolysaccharide-induced acute lung injury in mice. *Respiration* 81: 39–46, 2011. doi:10.1159/000319151.

42. **Mabley J**, **Gordon S**, **Pacher P.** Nicotine exerts an anti-inflammatory effect in a murine model of acute lung injury. *Inflammation* 34: 231–237, 2011. doi:10.1007/s10753-010-9228-x.

43. **Sitapara RA**, **Gauthier AG**, **Valdés-Ferrer SI**, **Lin M**, **Patel V**, **Wang M**, **Martino AT**, **Perron JC**, **Ashby CR Jr**, **Tracey KJ**, **Pavlov VA**, **Mantell LL.** The α7 nicotinic acetylcholine receptor agonist, GTS-21, attenuates hyperoxia-induced acute inflammatory lung injury by alleviating the accumulation of HMGB1 in the airways and the circulation. *Mol Med* 26: 63, 2020. doi:10.1186/s10020-020-00177-z.

44. **Su X**, **Matthay MA**, **Malik AB.** Requisite role of the cholinergic α7 nicotinic acetylcholine receptor pathway in suppressing gram-negative sepsis-induced acute lung inflammatory injury. *J Immunol* 184: 401–410, 2010. doi:10.4049/jimmunol.0901808.

45. **Boland C**, **Collet V**, **Laterre E**, **Lecuivre C**, **Wittebole X**, **Laterre PF.** Electrical vagus nerve stimulation and nicotine effects in peritonitis-induced acute lung injury in rats. *Inflammation* 34: 29–35, 2011. doi:10.1007/s10753-010-9204-5.

46. **Giebelen IA**, **Leendertse M**, **Florquin S**, **van der Poll T.** Stimulation of acetylcholine receptors impairs host defence during pneumococcal pneumonia. *Eur Respir J* 33: 375–381, 2009. doi:10.1183/09031936.00103408.

47. **Inoue T**, **Abe C**, **Sung SS**, **Moscalu S**, **Jankowski J**, **Huang L**, **Ye H**, **Rosin DL**, **Guyenet PG**, **Okusa MD.** Vagus nerve stimulation mediates protection from kidney ischemia-reperfusion injury through α7nAChR+ splenocytes. *J Clin Invest* 126: 1939–1952, 2016. doi:10.1172/JCI83658.

48. **Tracey KJ.** Physiology and immunology of the cholinergic antiinflammatory pathway. *J Clin Invest* 117: 289–296, 2007. doi:10.1172/JCI30555.

49. **Venosa A**, **Malaviya R**, **Gow AJ**, **Hall L**, **Laskin JD**, **Laskin DL.** Protective role of spleen-derived macrophages in lung inflammation, injury, and fibrosis induced by nitrogen mustard. *Am J Physiol Lung Cell Mol Physiol* 309: L1487–L1498, 2015. doi:10.1152/ajplung.00276.2015.

50. **Andres-Hernando A**, **Okamura K**, **Bhargava R**, **Kiekhaefer CM**, **Soranno D**, **Kirkbride-Romeo LA**, **Gil HW**, **Altmann C**, **Faubel S.** Circulating IL-6 upregulates IL-10 production in splenic CD4+ T cells and limits acute kidney injury-induced lung inflammation. *Kidney Int* 91: 1057–1069, 2017. doi:10.1016/j.kint.2016.12.014.

51. **Klein CL**, **Hoke TS**, **Fang WF**, **Altmann CJ**, **Douglas IS**, **Faubel S.** Interleukin-6 mediates lung injury following ischemic acute kidney injury or bilateral nephrectomy. *Kidney Int* 74: 901–909, 2008. doi:10.1038/ki.2008.314.

52. **Teixeira JP**, **Ambruso S**, **Griffin BR**, **Faubel S.** Pulmonary consequences of acute kidney injury. *Semin Nephrol* 39: 3–16, 2019. doi:10.1016/j.semnephrol.2018.10.001.

53. **Yue Y**, **Liu R**, **Cheng W**, **Hu Y**, **Li J**, **Pan X**, **Peng J**, **Zhang P.** GTS-21 attenuates lipopolysaccharide-induced inflammatory cytokine production in vitro by modulating the Akt and NF-κB signaling pathway through the α7 nicotinic acetylcholine receptor. *Int Immunopharmacol* 29: 504–512, 2015. doi:10.1016/j.intimp.2015.10.005.

54. **Kielar ML**, **John R**, **Bennett M**, **Richardson JA**, **Shelton JM**, **Chen L**, **Jeyarajah DR**, **Zhou XJ**, **Zhou H**, **Chiquett B**, **Nagami GT**, **Lu CY.** Maladaptive role of IL-6 in ischemic acute renal failure. *J Am Soc Nephrol* 16: 3315–3325, 2005. doi:10.1681/ASN.2003090757.

55. **Kooguchi K**, **Hashimoto S**, **Kobayashi A**, **Kitamura Y**, **Kudoh I**, **Wiener-Kronish J**, **Sawa T.** Role of alveolar macrophages in initiation and regulation of inflammation in *Pseudomonas aeruginosa* pneumonia. *Infect Immun* 66: 3164–3169, 1998. doi:10.1128/IAI.66.7.3164-3169.1998.

56. **Madjdpour C**, **Jewell UR**, **Kneller S**, **Ziegler U**, **Schwendener R**, **Booy C**, **Kläusli L**, **Pasch T**, **Schimmer RC**, **Beck-Schimmer B.** Decreased alveolar oxygen induces lung inflammation. *Am J Physiol Lung Cell Mol Physiol* 284: L360–L367, 2003. doi:10.1152/ajplung.00158.2002.

57. **Nakamura T**, **Abu-Dahab R**, **Menger MD**, **Schäfer U**, **Vollmar B**, **Wada H**, **Lehr CM**, **Schäfers HJ.** Depletion of alveolar macrophages by clodronate-liposomes aggravates ischemia-reperfusion injury of the lung. *J Heart Lung Transplant* 24: 38–45, 2005. doi:10.1016/j.healun.2003.10.007.

58. **Beck-Schimmer B**, **Schwendener R**, **Pasch T**, **Reyes L**, **Booy C**, **Schimmer RC.** Alveolar macrophages regulate neutrophil recruitment in endotoxin-induced lung injury. *Respir Res* 6: 61, 2005. doi:10.1186/1465-9921-6-61.

59. **Frank JA**, **Wray CM**, **McAuley DF**, **Schwendener R**, **Matthay MA.** Alveolar macrophages contribute to alveolar barrier dysfunction in ventilator-induced lung injury. *Am J Physiol Lung Cell Mol Physiol* 291: L1191–L1198, 2006. doi:10.1152/ajplung.00055.2006.

60. **Sabatel C**, **Radermecker C**, **Fievez L**, **Paulissen G**, **Chakarov S**, **Fernandes C**, **Olivier S**, **Toussaint M**, **Pirottin D**, **Xiao X**, **Quatresooz P**, **Sirard JC**, **Cataldo D**, **Gillet L**, **Bouabe H**, **Desmet CJ**, **Ginhoux F**, **Marichal T**, **Bureau F.** Exposure to bacterial CpG DNA protects from airway allergic inflammation by expanding regulatory lung interstitial macrophages. *Immunity* 46: 457–473, 2017. doi:10.1016/j.immuni.2017.02.016.

61. **van Rooijen N**, **Hendrikx E.** Liposomes for specific depletion of macrophages from organs and tissues. *Methods Mol Biol* 605: 189–203, 2010. doi:10.1007/978-1-60327-360-2_13.